

반복하중을 받는 철근콘크리트 기둥부재의 재료 및 기하적인 비선형 해석

Material and Geometrical Nonlinear Analysis of Reinforced Concrete Columns under Cyclic Loading

유영화* 김운학** 신현목***
Yoo, Young Hwa Kim, Woon Hak Shin, Hyun Mock

국문요약

이 연구에서는 반복적인 횡하중이 작용하고 있는 철근콘크리트 기둥의 비선형 이력거동 및 파괴거동을 해석적으로 예측할 수 있는 기법을 제시하였다. 하중의 단계에 따라 수반하게 되는 콘크리트의 균열 및 철근의 항복, 이로 인한 부착 효과와 골재의 맞물림 현상 및 강도의 감소 등과 같은 특성을 고려한 재료적 비선형성을 고려하였고, 기둥부재에 일반적으로 배치되는 구속철근으로 인한 강도의 증가 효과를 고려하였다. 여기서, 철근콘크리트의 응력-변형도 관계는 분산균열모델에 기초하여 평균값으로 표현된다. 비교적 큰 압축하중과 함께 지진하중과 같이 큰 규모의 횡하중으로 인한 대변위 문제를 고려할 수 있도록 total Lagrangian formulation에 의한 기하적인 비선형성을 고려하였다. 본 연구에서 작성한 유한요소 해석 프로그램에 의한 결과를 다른 연구자의 실험 결과와 비교함으로써 본 연구에서 제시한 해석기법의 타당성을 검증하였다.

주요어 : 이력거동, 대변위 문제, total Lagrangian formulation

ABSTRACT

This paper presents an analytical prediction of the hysteresis behavior of reinforced concrete long column with rectangular section under the cyclic loading state. The mechanical characteristic of cracked concrete and reinforcing bar in concrete has been modeled, considering the bond effect between reinforcing bar and concrete, the effect of aggregate interlocking at crack surface and the stiffness degradation after the crack has taken place. The strength increase of concrete due to the lateral confining reinforcement has been also taken into account to model the confined concrete. The formulation of these models for concrete and reinforcing bar has been based on the smeared crack concept that the stress-strain relationship of reinforced concrete element would be defined using the average values. In addition to the material nonlinear properties, the algorithm for large displacement problem that may give an additional deformation has been formulated using total Lagrangian formulation. The analytically predicted behavior was compared with test result and they showed good agreement in overall behavior.

Key words : hysteresis behavior, large displacement problem, total Lagrangian formulation

1. Introduction

Reasonably close identification of an inelastic and hysteretic response of the reinforced con-

crete structure and its adequate analytical modeling can be indeed a difficult practice because of its nonlinear and an-isotropic properties. An analytical approach by finite element method produces reliable result, provided that the constitutive models for reinforced concrete would represent its real characteristic of the mechanical behavior. In this paper,

* 정희원 · 성균관대학교 토목공학과 박사과정 수료

** 정희원 · 국립 한경대학교 토목공학과 조교수, 공학박사

*** 정희원 · 성균관대학교 토목공학과 교수, 공학박사

본 논문에 대한 토의를 6월 30일까지 학회로 보내 주시면 그 결과를 게재하겠습니다.

the material nonlinearity with confining effect of the lateral reinforcement and geometric nonlinearity based on total Lagrangian formulation⁽¹⁾ were taken into account to predict an inelastic behavior of the reinforced concrete column.

It is generally assumed that the reinforcing bar in the reinforced concrete element resists forces only in axial direction. Base on this assumption, the stress and strain of the reinforcing bar can be obtained using truss (or line) element regarding as an independent element. The formulation of reinforcing bar using truss element is effective, particularly when the structural behavior is governed by reinforcing bar.

The reinforcing bar in the reinforced concrete is generally distributed in orthogonal direction and several distributed cracks are assumed to occur. Thus it is appropriate to consider the overall behavior after the crack develops rather than the initiation and propagation of each crack. The analytical models for the reinforced concrete element are described using the smeared crack approach that is regarding the tributary area with several cracks and reinforcing bars as a finite continuum element⁽²⁾, where the constitutive equations are expressed using the average stress and the average strain relationship. The material models employed in this paper are based on the multi-directional orthotropic models whose reference coordinates are set to the cracks.

2. Nonlinear material models

The reinforced concrete can efficiently be expressed as the superposition of the concrete and reinforcing bar. However, the reinforced concrete is not of simply adding each of these

analytical models but of properly combining each of them, recognizing that there exists a bond effect between the concrete and the reinforcement. Hence, an analytical model of concrete and reinforcing bar in the reinforced concrete should be considered independently.

2.1 Modeling of uncracked concrete and cracking criteria

The Elasto-Plastic and Fracture model⁽³⁾ for the biaxial state of stress was used as a constitutive equations of uncracked concrete. Using this model, the nonlinearity and anisotropy of the concrete can be expressed regardless of the loading history including strain-softening domain. In this model, the equivalent stress-strain relation is formulated using the initial elastic modulus, the fracture parameter and equivalent plastic strain. The equivalent plastic strain is defined as a strain when the stress is reversed to zero. The fracture parameter indicates the degradation of stiffness in unloading process. The equivalent plastic strain and the fracture parameter are not changed unless the equivalent strain exceeds the maximum strain previously reached.

It was assumed in this paper that the crack takes place when the principle tensile strain ϵ_t reaches the cracking strain ϵ_{cr} and this value represents the principle tensile strain when the stress of concrete reaches the fracture envelope. In this paper, Niwa model⁽⁴⁾ for the compression-tension domain and Aoyagi-Yamada model⁽⁵⁾ for the tension-tension domain were used respectively as the fracture envelopes under the biaxial state of stresses (Fig. 1), where σ_1, σ_2 are the principal stresses and σ'_t, σ_c are the uniaxial tensile and compressive strength of concrete, respectively.

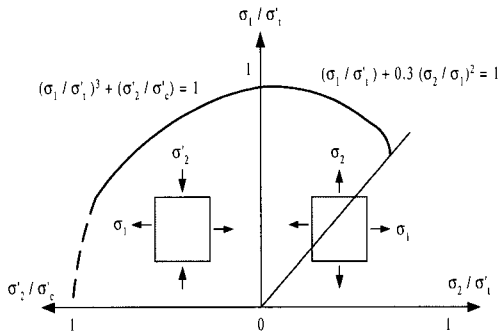


Fig. 1 Cracking stress criteria for 2-D stress state

It is assumed in the smeared crack concept that the first crack perpendicular to the principle tensile stress takes place when the principle stress of concrete at the gauss integration point reaches the fracture envelope. By the way, a new crack appears in a direction different from that of existing crack under the reversed cyclic loading. But it can hardly be treated as a new crack when the angle between them is less than 15 degrees.⁽⁶⁾ Hence, this paper assumed that the second crack does not take place even when the tensile stress has reached the fracture envelope. The cracking criterion for the second crack is assumed to be same as the first crack.

2.2 Modeling of cracked concrete

2.2.1 Modeling of concrete normal to crack

An anisotropic property becomes significant after the crack has taken place in concrete and the stress-strain relationship takes on an orthogonal anisotropy in the direction normal to crack. This means that the stress-strain relations have to be modeled in the direction parallel as well as normal to crack and in the shear direction, respectively. The cracked reinforced concrete element can be modeled using the tension stiffness model representing

the tension stiffening effect of concrete caused by the bond effect between the concrete and reinforcing bar. Okamura *et. al.*⁽⁷⁾ have developed an average stress-average strain relationship of concrete normal to crack from the test result for monotonic loading. But they overlooked the fact that the tensile stress resisted by the concrete results from the bond effect between the concrete and reinforcing bar and tried to express the tension stiffening effect of concrete as simple as possible.

Hence, it may cause an inaccuracy of the analysis results under the complicated stress distribution, especially when the reinforcing ratios in orthogonal directions show a significant discrepancy. The tension stiffness model proposed by Okamura *et. al.* has been modified in this paper. The bond model has been used to obtain the tensile stresses of concrete in each direction of the reinforcing bar, and then the tensile stresses of concrete has been transformed to those in the directions of reinforcing bars. Using this process, the tension stiffening effect of concrete could be considered more realistically.

For unloading and reloading, the model proposed by Tamai *et al.* was basically used.⁽⁸⁾ They performed a reversed cyclic loading test to present the tension stiffness model regarding the stresses in concrete as the sum of the stresses from the bond action with reinforcing bars and those from the contact at crack plane.

The unloading process brings about closing of crack that has taken place. But it should be noted that the two surfaces of crack start contacting each other even before the average strain ϵ_{x0} of concrete becomes zero. Hence, 150×10^{-6} has been given as the strain when the crack surfaces start contacting (Fig. 2).

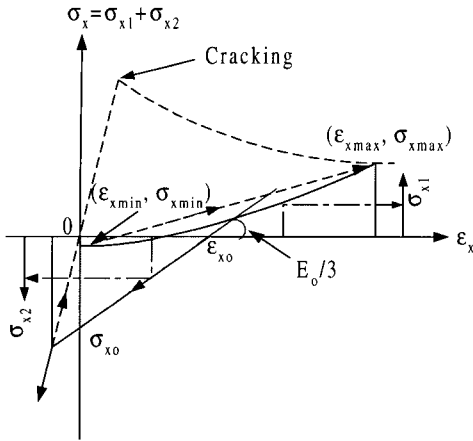


Fig. 2 Tension stiffness model for unloading and reloading

2.2.2 Modeling of concrete parallel to crack

The Modified Elasto-Plastic Fracture Model⁽⁷⁾ was used in this paper as a model for concrete under the compressive stress. This model describes the degradation in compressive stiffness by modifying the fracture parameter in terms of the strain perpendicular to the crack plane. The main reason for the degradation in the stiffness of cracked concrete may be attributed to the fact that the ability of concrete carrying a compressive stress is degraded in the vicinity of crack on account of the roughness of crack surfaces. This effect cannot keep increasing for every large cracks. Therefore, the value of degradation factor has a minimum limit. The ratio of the fracture parameter K' for the cracked concrete to K_0 for the uncracked concrete is given as

$$K' = \omega K_0 \quad (1)$$

where K' : fracture parameter of the cracked concrete

K_0 : fracture parameter of the uncracked concrete

ω : function of the strain perpendicular to the crack plane

ε_x : strain perpendicular to the crack plane

Therefore, the compressive model for the cracked concrete is given as

$$\sigma_y = E_o K' (\varepsilon_y - \varepsilon_p) \quad (2)$$

where E_o : secant modulus of concrete (kg/cm^2)

ε_y : strain parallel to the crack plane

ε_p : plastic strain parallel to the crack plane

For unloading and reloading, the same model based on the Elastic-Plastic and Fracture Model was also used. Since the fracture in the inner part of the envelope, in other words, at unloading and reloading is not progressive when referred to the basic concept of the Elastic-Plastic and Fracture Model, the fracture parameter and plastic strain show a linear behavior. This means that the energy is not consumed during unloading and reloading process. Hence the calculation procedure becomes simple if assumed that the energy consumption by the compressive deformation of concrete is much less than the total energy consumption. But it should be noted that in case of high compressive stress acting on the concrete, the energy consumption by the compressive deformation of concrete can not be neglected when compared with total energy consumption.

It is necessary to model the damage of the inner concrete under the cyclic loading to reasonably consider the energy consumption during unloading and reloading. This paper assumed for the simplicity that the energy consumption is considered by modifying the

stress-strain curve at unloading to an arc shape whose tangential stiffness becomes infinite and passing through the point of residual strain (Fig. 3).^{(10),(11)}

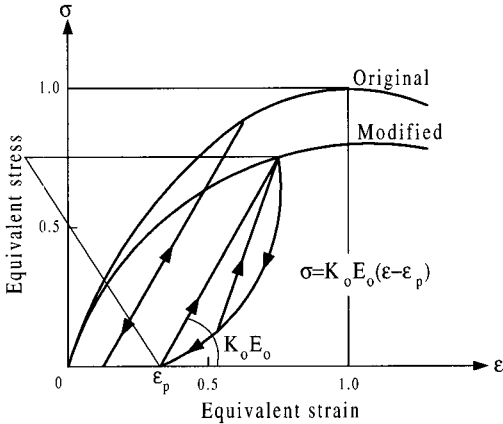


Fig. 3 Equivalent stress-equivalent strain relationship

2.2.3 Modeling of concrete in shear direction

In order to consider the effect of shear stress transfer due to the aggregate interlocking at crack surface, the shear transfer model based on the Contact Surface Density Function $Z(\omega, \delta, \theta_s)$ ⁽¹²⁾ was basically used (Fig. 4). Since this model defines the form of the crack surface in terms of three parameters (crack width, slip and its ratio) and assumes the contact surface to respond elasto-plastically,

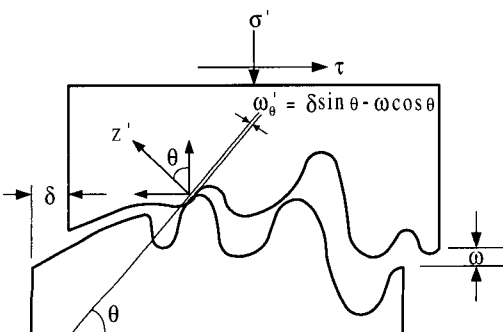


Fig. 4 Shear transfer at crack surface

it is applicable to the arbitrary loading history. This model defines the shear and compressive stress at crack surface as

$$\tau = \int_{-\pi/2}^{+\pi/2} [Z(\omega, \delta, \theta_s) \sin \theta_s] d\theta_s \quad (3)$$

$$\sigma = \int_{-\pi/2}^{+\pi/2} [Z(\omega, \delta, \theta_s) \cos \theta_s] d\theta_s \quad (4)$$

Li *et al.* have obtained the integral solutions for the monotonic loading from the above model, ignoring both the elastic components in total deformation at crack plane and the effect of crack width. And Shin *et al.* have developed a simple shear transfer model for unloading and reloading by performing the parametric numerical analysis for the various loading history.⁽¹⁰⁾

2.3 Modeling of reinforcing bar

The stress acting on the reinforcing bar embedded in concrete is not uniform, but it takes the maximum values where the bar is exposed to a crack plane. The constitutive model can be set equal to that for the bare bar if the stress-strain relation is elastic. However, the elastic relationship between the average steel stress and steel strain is lost as soon as the bar yields at crack plane, even if it remains unyielded elsewhere. And the average steel stress at that instance is lower than its yield strength.⁽⁸⁾ In this paper the bilinear model⁽¹⁰⁾ derived for the post-yielding model of a bar was used in the formulation under the state of loading.

An elastic relationship still holds between the average steel stress and steel strain through any unloading and reloading operations before the bar has yielded, since the bar remains in an elastic range. However, an elastic relationship

is lost when the bar has yielded, and the average steel stress-average steel strain relationship also becomes nonlinear.

The average steel stress-average steel strain relationship at unloading or reloading can be determined if the stress distribution of bar between the cracks and the stress-strain relation for the bare bar has been determined for that mode of loading. Kato's model⁽¹³⁾ for the bare bar under the reversed cyclic loading and the assumption of stress distribution expressed by a cosine curve were used in calculating the mechanical behaviors of reinforcing bars in concrete under the reversed cyclic loading.

This method required a great deal of computation time. Hence he developed a simpler model for the average stress-strain relation of post-yielding steel by taking the stress and strain of Kato's bar as the average stress and strain of steel, respectively.⁽¹⁰⁾ In this paper, Modified Kato's model was used as a post-yield steel model for unloading and reloading loops.

2.4 Modeling of confining effects

A transverse reinforcement is provided to confine the compressed concrete within the core region and to prevent buckling of the longitudinal reinforcement. The reinforced concrete column confined by the transverse reinforcement shows an improved ultimate strength and strain capacity.^{(3),(14),(15)} It also has a superior ductile capacity to the unconfined concrete. This paper has taken the confining effects of the transverse reinforcement into account by modifying the compressive stress-strain model of unconfined concrete. It was formulated in terms of the amount of the

longitudinal and transverse reinforcement, and the yield strength and distribution type of the transverse reinforcement. In order to consider the confining effects, the effective confining stress and effective confining coefficient have been evaluated for the arbitrary cross sectional shape. The spalling of the cover concrete and the buckling of the axial reinforcement have been neglected in this paper.

In this model, the compressive strength f_{cc}' of the confined circular or rectangular sections with equal effective confining stress f_l' in the orthogonal directions is related to the unconfined strength f_c' by the relationship.

$$K_{cc} = \frac{f_{cc}'}{f_c'} = \left(-1.254 + 2.254 \sqrt{1 + \frac{7.94f_l'}{f_c'}} - \frac{2f_l'}{f_c'} \right) \quad (5)$$

and the peak stress is attained at a strain of

$$\epsilon_{cc} = 0.002[1 + 5(f_{cc}'/f_c' - 1)] \quad (6)$$

3. Finite element analysis with large displacements

In addition to the material nonlinear properties in the previous sections, large displacement problem that may be significant in the case of long column has been taken into account in the nonlinear finite element analysis based on total Lagrangian formulation. It makes use of Green-Lagrange strain tensors and the second Piola-Kirchhoff stress tensors.

The basic equilibrium equation including the large deformations and material nonlinearity takes on nonlinear relationship and its solution cannot be solved directly. An approximate

solution can be obtained by referring all variables to a previously calculated known equilibrium configuration and linearizing the resulting equation. This solution can then be improved by iteration.

Eight-node and two-node isoparametric plane stress element with two-degree of freedom in each node were used in the displacement-based element formulation of the reinforced concrete and reinforcing bar, respectively (Fig. 5). They have been numerically integrated using 3-and 1-point Gauss rule, respectively and all finite element matrices have been defined at Gauss Integration point.⁽¹⁾

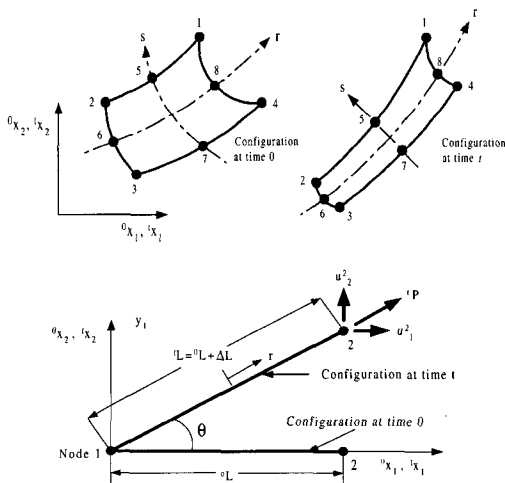


Fig. 5 Isoparametric finite elements representing reinforced concrete and reinforcing bar element

A truss (or line) element is a structural member capable of transmitting stresses only in the direction normal to the cross section. Thus, in total Lagrangian formulation only the corresponding longitudinal strain needs to be considered. Since all derivatives of interpolation functions are with respect to the initial coordinate system in Total Lagrangian formulation, they are calculated only once in the first

load step, and stored on back-up storage for use in all subsequent load steps.

The equilibrium equation of the system at each load step requires iterative procedure to obtain the solutions within convergence tolerance. The Newton-Raphson, Modified Newton-Raphson and Initial Stiffness method have been used appropriately as an iterative procedure. And the Crout's decomposition algorithm has been used to obtain the solution vectors of the system.

The analytical program developed in this paper is composed of pre-processor, DRPR and main-processor, DRPT that are the modified version of RCSDA and RCSDC, respectively.⁽¹⁶⁾ The program DRPT has been developed for material and geometrical nonlinear dynamic analysis of RC structure modeled as two-dimensional plane stress element under in-plane loading state. But the dynamic analysis option is currently under development. It has been devised for users to select an analysis option corresponding to the type of analysis, for examples, static or dynamic and geometrically linear or nonlinear analysis, etc.

The pre-processor DRPR reads input data and to make skyline index, restraint factors, linear strain-displacement matrix, and restart preparation. All data needed to execute a main analysis are restored to external files using the technique of dynamic data allocation. The main processor DRPT reads nodal forces or nodal displacements, incremental loads and indices for structuring the total matrix, and performs the analysis using the element data stored in external files. The stored data including stress and strain history of each element are also necessary for restart function in which is convenient for nonlinear and dynamic analysis.

4. Verification of present analytical method

The ten full-scale column specimens with square cross sections⁽¹⁷⁾ were analyzed for verifying the analytical method of this paper. Fig. 6 and 7 show overall dimensions and reinforcement arrangement on the test specimens, respectively. Each complete column has a cross section 457×457 mm and a height of 350.52 cm. The beam stub is provided for application of lateral load and strengthening of the joint region. The height of the upper column is larger than the lower column, and additional reinforcement is provided in the lower column except in specimen NC-1.

Design compressive strength of concrete is 433.2 kg/cm^2 and yield stress of vertical and transverse reinforcement is 4221.6 kg/cm^2 , respectively. Details on the test specimens are described in Table 1. Vertical reinforcement consisted of eight bars with 25.4 mm diameters providing a reinforcement ratio of 0.0195.

Fig. 8 shows a loading arrangement. Applied vertical load P_v is listed in table 1 and kept constant during the entire loading cycles. Then the lateral load is applied with hydraulic rams pushing against reaction frames.

Test specimens was modeled using the plane stress element with 8-node and the truss element with 2-node in the finite element analysis. And the vertical reinforcement was modeled using the truss element and the transverse reinforcement was modeled in RC element with distributed reinforcement, respectively. It was assumed in this paper that the element loaded is not failed by compression.

Fig. 9 shows load-displacement relation of specimen NC-2 from test and analysis of

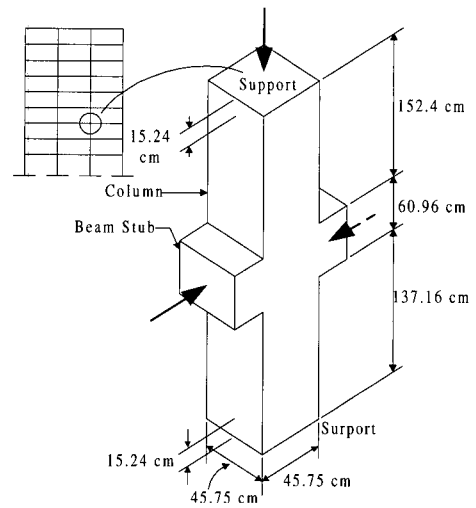


Fig. 6 Overall view of test specimen

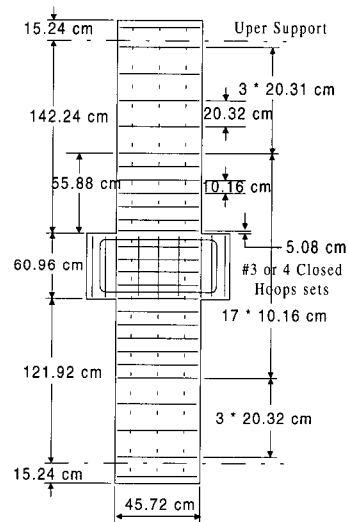


Fig. 7 Reinforcement details

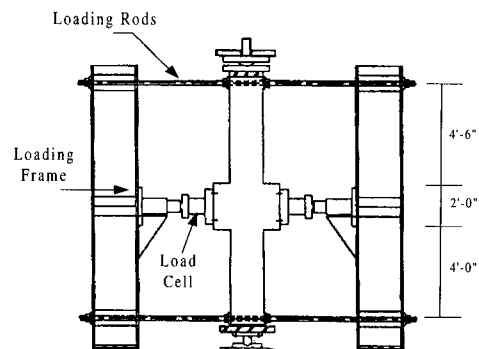


Fig. 8 Loading arrangement

Table 1 Details of test variables

Specimens	Vertical load		Transverse reinforcement			
	P_v/P_o ①	ton	D(cm)	A_{sh} cm ²	σ_y kg/cm ²	ρ (%)
NC-2	0.2	172.4	1.27	4.387	4221.6	2.19
NC-3	0.4	353.8	1.27	4.387	4221.6	2.19
NC-4	0.3	263.1	0.95	2.451	4221.6	1.26
NC-5	0.3	260.8	1.27	4.387	4221.6	2.19
NC-6	0.3	235.9	1.27	2.580	4221.6	1.29
NC-7	0.3	244.9	1.27	2.580	4221.6	1.29
NC-8	0.3	254.0	1.27	4.387	4221.6	2.19
NC-9 ⁽²⁾	0.3	240.4	1.27	2.580	4221.6	1.29
NC-10 ⁽³⁾	0.3	249.5	0.95	1.419	4221.6	1.29
NC-12	0.3	251.3	0.95	1.935	4221.6	1.29

- ① $P_o = 0.85\sigma_c(A_g - A_{st}) + A_{st}\sigma_y$; P_v =Vertical load
- ② specimen with no cross tie and continuous square hoop at 100 mm pitch
- ③ specimen with no cross tie and continuous square hoop at 57 mm pitch

this paper neglecting geometrical nonlinear effect. The behavior after peak strength is a little overestimated when compared with Fig. 10 in which geometrical nonlinear effect is included. The maximum value of lateral shear force obtained from analysis shows good agreement with test result, as shown in Fig. 10, and the overall behavior is also much closer to test result. Fig. 11 shows a deformed shape in the final load step and Fig. 12 is the failure pattern by test and analysis.

Fig. 13 and 14 are load-displacement curves of specimen NC-4. The high axial force corresponding to 30% of calculated ultimate strength is acting on it.

It is well known that the lateral displacement of the head of a column relative to its base give rise to second order effect (P-Δ effect). The post yield branch has a negative slope due to the presence of P-Δ effect and is more pronounced in the column with higher level of axial loading. The rapid degradation of strength after peak due to P-Δ effect by

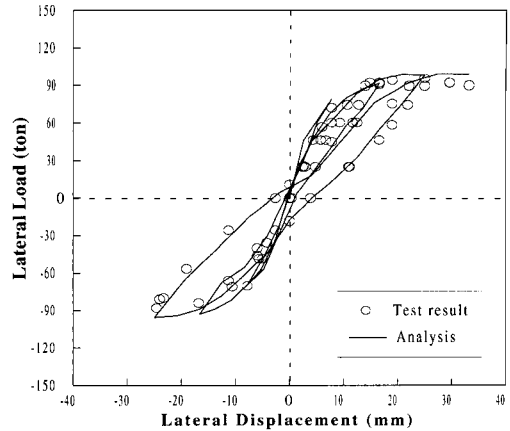


Fig. 9 Load-displacement curve for NC-2 (Material nonlinear only)

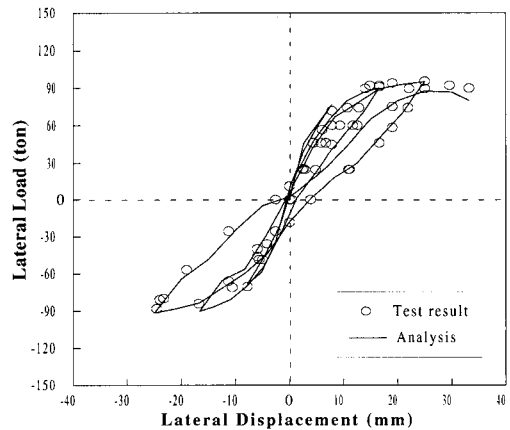


Fig. 10 Load-displacement curve for NC-2 (Material and geometric nonlinear)

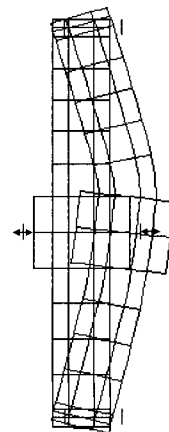


Fig. 11 Deformed shape of NC-2

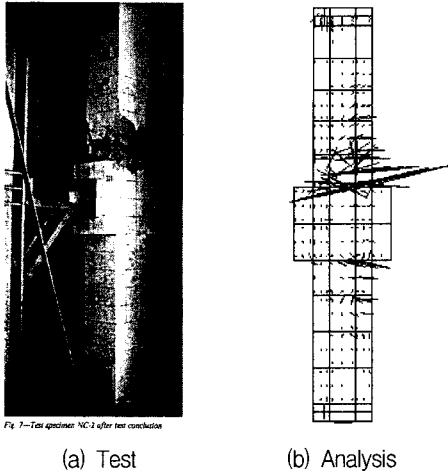


Fig. 12 Failure pattern for Specimen NC-2

large axial force is shown in Fig. 14. Hence, relatively low levels of axial loading have a favorable effect on the seismic performance of reinforced concrete columns as they increase their energy dissipation capacities. However high levels of axial loading may drastically reduce the ductility of columns after peak and they induce failure modes that may lead to partial or total collapse of the structure. The maximum lateral loads by test and analysis of the total test specimens are compared in Table 2 and the result by analysis shows good agreement with test result.

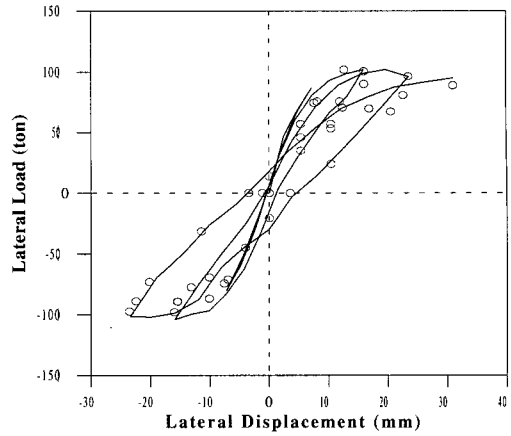


Fig. 13 Load-displacement curve for NC-4 (Material nonlinear only)

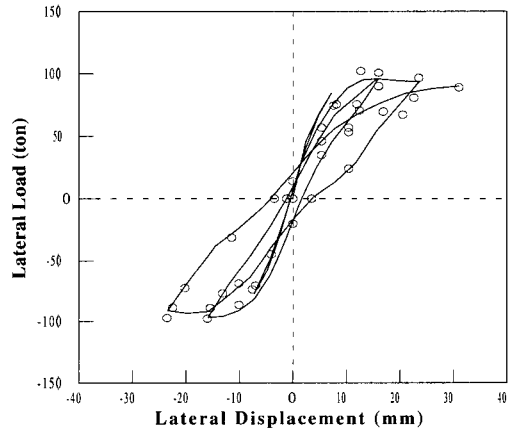


Fig. 14 Load-displacement curve for NC-4 (Material and geometric nonlinear)

Table 2 Comparison of maximum horizontal load (unit : ton)

Specimen	Calculated (1) ⁽¹⁷⁾	Measured (2) ⁽¹⁷⁾	This study		
			(3)	(4)	(4)/(3)
NC-2	83.9	95.3	99.1	95.1	0.96
NC-3	86.2	106.6	122.3	112.8	0.92
NC-4	89.8	102.0	102.0	95.9	0.94
NC-5	88.9	104.3	113.0	105.0	0.93
NC-6	81.6	63.5	104.9	99.2	0.95
NC-7	84.8	97.5	105.4	100.4	0.95
NC-8	87.1	90.7	111.6	104.7	0.94
NC-9	82.1	97.5	105.3	99.7	0.95
NC-10	84.8	95.3	107.3	100.6	0.94
NC-12	85.3	88.5	101.5	97.9	0.96

① ACI318-83 neglecting P-Δ effect ; (2) Test result

② Material nonlinear only ; (4) Material and geometric nonlinear

5. Conclusions

1. This paper presented an analytical prediction for the behavior of reinforced columns and the result was compared with test result.
2. Modeling the axial reinforcement as an independent truss element resulted in better overall behavior.
3. The maximum lateral strength was decreased by 4 to 8 percents due to P- Δ effect and this effect could be described by considering large displacement problem based on total Lagrangian formulation.
4. An analytical approach of this paper could describe the overall behavior with high accuracy, including the strength increase due to the confining reinforcement and the strength decrease due to the large displacement effect.

Acknowledgement

This work was supported by the Korea Science and Engineering Foundation (KOSEF) through the Earthquake Engineering Research Center at Seoul National University.

Reference

1. Bathe, K. J., *Finite Element Procedures*, Prentice-Hall, 1996.
2. COMITE EURO-INTERNATIONAL DU BETON, *RC ELEMENTS UNDER CYCLIC LOADING, STATE OF THE ART REPORT*, CEB, 1996
3. Maekawa, K. and Okamura, H., "The deformational behavior and constitutive equation of concrete using elasto-plastic and fracture Model," *Journal of faculty of engineering*, The University of Tokyo, Vol. 37, No. 2, 1983, pp. 253-328.
4. Niwa, J., *Mechanical Characteristic of Reinforced Concrete Plate Element (In Japanese)*, The University of Tokyo, 1980.
5. Aoyagi, Y. and Yamada, K., "Strength and deformation characteristics of reinforced concrete shell elements subjected to in-plane forces," *Proceeding of JSCE*, No. 331, 1983, pp. 167-180.
6. Yoo, Y. H., Choi, J. H., and Shin, H. M., "Inelastic analysis of reinforced concrete structure subjected to cyclic loads with confining effects of lateral tie," *Journal of Earthquake Engineering Society of Korea*, Vol. 2, No. 1, 1998, pp. 79-92.
7. Okamura, H., Maekawa, K., and Izumo, J., "RC plate element subjected to cyclic loading," *IABSE Colloquium Delft*, Vol. 54, 1987, pp. 575-590.
8. Shima, H. and Tamai, S., "Tension stiffness model under reversed loading including post yield range," *IABSE Colloquium Delft*, 1987, pp. 547-556.
9. Shima, H., Chou, L., and Okamura, H., "Micro and macro models for bond behavior in reinforced concrete," *Journal of the faculty of engineering*, The University of Tokyo (B), Vol. 39, No. 2, 1987, pp. 133-194.
10. Shin, H., "Finite Element Analysis of Reinforced Concrete Members Subjected to Load Reversals," Ph. D. Thesis, The University of Tokyo, 1988.
11. Okamura, H. and Maekawa, K., *Nonlinear Analysis and Constitutive Models of Reinforced Concrete*, Gihodo-Shuppan, Tokyo, 1990.
12. Li, B. and Maekawa, K., "Contact density model for stress transfer across cracks in

- concrete," *Concrete Engineering*, JCI, Vol. 26, No. 1, 1988.
13. Kato, B, "Mechanical Properties of Steel under Load Cycles Idealizing Seismic Action," *Bulletin D'Information No. 131*, CEB, AICAP-CEB symposium, Rome, 1979, pp. 7-27.
14. Sheikh, S. A. and Uzumeri, S. M., "Strength and ductility of tied concrete columns," *Journal of the Structural Division*, ASCE, Vol. 106, ST5, May 1980, pp. 1079-1102
15. Mander, J. B., Priestley, M. J. N., and R. Park, "Theoretical stress-strain model for confined concrete," *Journal of the Structural Division*, ASCE, Vol. 114, No. 8, August 1988, pp. 1804-1826.
16. Korea Science and Engineering Foundation (KOSEF), "A study on the material damage, failure and collapse behaviors of civil structure," 94-0600-01-01-3, Oct. 1997.
17. Azizinamini, A., Corley, W. G., and Johal, L. S., "Effects of transverse reinforcement on seismic performance of columns," *ACI Structural Journal*, Vol. 89, No. 4, July-August 1992, pp. 442-450.